B1-based SAR Estimation for Human Brain Imaging with Average Brain Property Values Substitution

Xiaotong Zhang[1], Jiaen Liu[1], Sebastian Schmitter[2], Pierre-Francois Van de Moortele[2], and Bin He[1]

[1]*Department of Biomedical Engineering, University of Minnesota, Minneapolis, MN, United States,* [2]*Center for Magnetic Resonance Research, University of Minnesota, Minneapolis, MN, United States*

Introduction: Recently proposed Electrical Properties Tomography (EPT) technique [1-3], which aims to reconstruct the electrical properties (EPs) of biological tissues via measured B1 maps, provides a feasible way for real-time quantitative and subject-specific SAR estimation. However, Laplacian operation over B1 is involved in all existing EPT algorithms, which may severely suffer from noise-contamination in measured B1, leading to deteriorated SAR estimation results. In the present study, using multi-channel coil array at 7T for brain imaging (healthy subjects), the performance has been evaluated when literature reported average electrical property and mass density (MD) values were employed as a substitution in local SAR calculation, intending for a more robust and reliable approach for SAR estimation.

Methods: Average brain conductivity (0.55 S/m), relative permittivity (51.95) and MD (1030 kg/m^3) at 7T (298 MHz) can be found at [4-5]. SEMCAD (Speag, Switzerland) was used with the Ella model (2×2×2mm^3) loaded in a reproduced 16-channel transceiver coil [6] (the head and neck portion placed supinely in the coil center). Both using simulated B1 distribution, the electric field as well as the subsequent voxel-wise (unaveraged) local SAR were calculated with target and average brain property values, respectively. In addition, a healthy volunteer was imaged with a 7T scanner (Siemens) equipped with the aforementioned coil [7-10]. With retrieved complex B1 distribution for each coil element [2], voxel-wise (unaveraged) local SAR was calculated by assuming a dominant $|\tilde{E}_z|$ compared to other electric field components (as described in [11]) and with average brain property values. Note that, since weak MRI signal observed in bone tissues is expected to deteriorate B1-mapping results, the present study was confined within soft brain tissues.

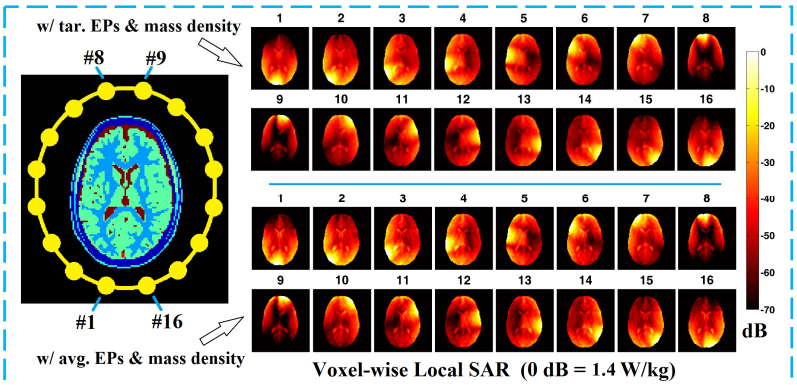

Fig. 1: On an axial slice (left, colors represent different tissue types), for each coil element, simulated voxel-wise SAR (in dB) with target (upper) and average (lower) brain property values, respectively.

Results: On a transverse slice of interest, SAR calculations (in dB) for each coil element were shown in Fig. 1, obtained with target and average brain property values, repectively. The average value substitution provides an overall +10.3% relative error (RE) and 0.991 correlation coefficient (CC) for all sixteen channels when compared with target results. Fig. 2 shows, on the central sagittal slice, the comparison of SAR (in dB) with coil element #16 as the transmitter, exhibiting +25.2% RE and 0.984 CC with the average value substitution; while on the central coronal slice with coil element #12 as the transmitter, +12.4% RE and 0.987 CC with the average value substitution. Fig. 3 depicts the comparison of peak SAR values on each transverse slice, illustrating a reasonably conservative SAR estimation (with up to +48.6% RE) by employing the average value substitution. Fig. 4 shows experiment result of SAR estimation (in dB) on a transverse slice of interest for selected channels, exhibiting reasonably similarity and visible brain structures as is observed in simulation results in Fig. 1.

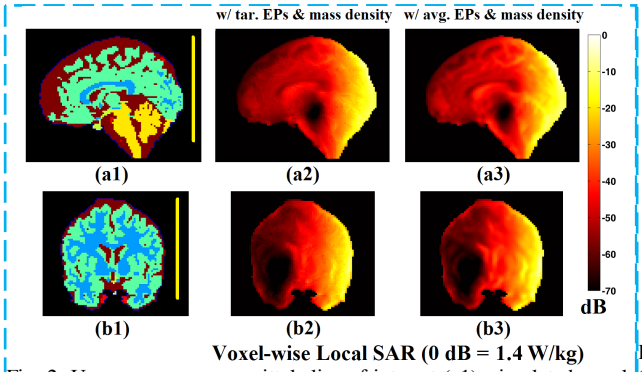

Fig. 2: Upper row – on a sagittal slice of interest (a1), simulated voxel-wise SAR (in dB) with target (a2) and average (a3) brain property values with coil element #16 as the transmitter. Lower row – on a coronal slice of interest (b1), simulated voxel-wise SAR with target (b2) and average (b3) brain property values with coil element #12 as the transmitter.

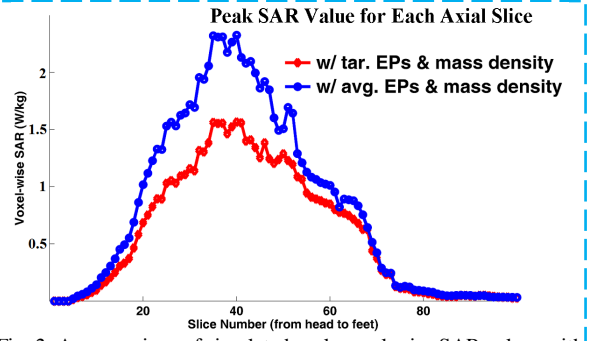

Fig. 3: A comparison of simulated peak voxel-wise SAR values with target (red) and average (blue) brain property values on each axial

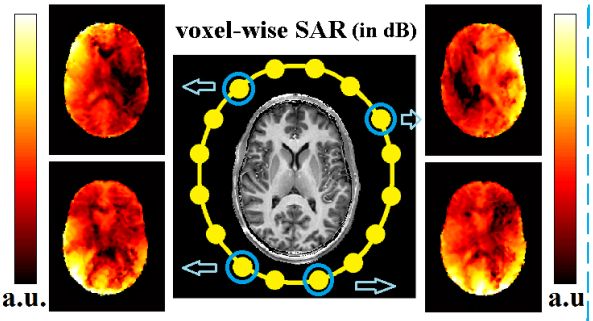

Fig. 4: Estimated voxel-wise SAR (in dB) for selected channels in human experiment at 7T..

Discussion and Conclusion: The computation of final SAR values is impacted by the propagation of experimental noise through the computation of at least three quantities: conductivity, relative permittivity and complex electric field. Based on reports in the literature, however, EPs values in the brain at a given frequency are fairly stable. The proposed method explicitly exploits this observation by attributing literature based average EPs and MD values to brain tissues, avoiding noise-sensitive second-order derivative steps; we experimentally demonstrate in a healthy volunteer at 7T that this approach stabilizes the performance of SAR computation, using nominal EPs and calculated E field (from retrieved complex B1). Naturally, a questionable aspect of this method is to assume negligible variations of brain property values, which comprises several components: variability between brain tissues, variability in different subjects and, most importantly, variability in pathological tissues. In healthy subjects, widely available segmentation software using standard T1w brain images provide the means of addressing tissue specific EPs and MD values. Robustness in case of pathological tissues will be a more critical question to evaluate that may require an additional step in the algorithm to determine on a case-per-case basis, based on (noisy) measured EPs, whether average reference values can be used as a proxy for the local EPs and MD. Such a decision-tree could be run for each region of the brain and deserves further study.

References: [1] Katscher et al., MRM 2012 (Online). [2] Zhang et al., MRM 2012 (Online). [3] Sodickson et al., ISMRM 2012, 387. [4] Gabriel et al., PMB 1996, 2251-2269. [5] http://transition.fcc.gov/oet/rfsafety/dielectric.html [6] Adriany et al., MRM 2008, 590-597. [7] Van de Moortele et al., MRM 2005, 1503-1518. [8] Van de Moortele et al., ISMRM 2007, 1676. [9] Van de Moortele et al., ISMRM 2009, 367. [10] Yarnykh, MRM 2007, 192-200. [11] Zhang et al., ISMRM 2012, 2669.

Acknowledgment: NIH R01 EB006433, R01 EB007920, R21 EB014353, T32 EB008389, P41 EB015894, S10 RR26783 and WM KECK Foundation.